2024 Sagan Exoplanet Summer Hybrid Workshop

Detecting Eclipse Timing Variation Planets with Other Methods

Ekrem M. Esmer
Department of Physics and McDonnell Center for the Space Sciences, Washington University, St. Louis, MO 63130, USA
McDonnell Center for the Space Sciences Postdoctoral Fellow
ekrem@wustl.edu
ORCID Link

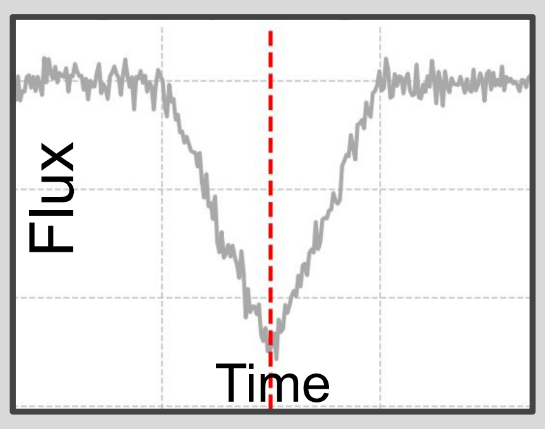

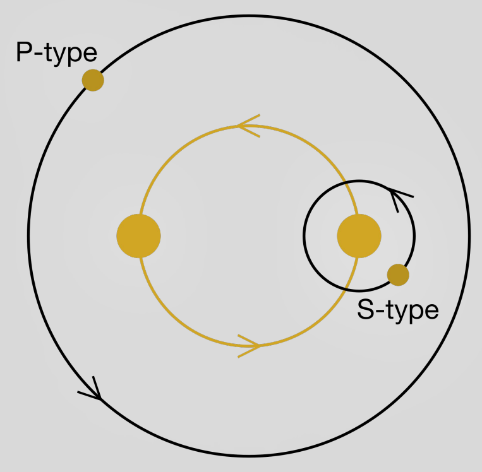

Eclipse Timing Variation Method

Eclipse Timing Variation (ETV) analysis is a method used to detect and characterize additional bodies in binary star systems. It involves precisely measuring the times of eclipses and looking for deviations from a constant period. These variations can indicate the gravitational influence of a third body, such as a planet or another star, causing the binary system to wobble. By analyzing these timing deviations, the presence, mass, and orbit of the additional objects can be inferred, even if they are not directly observable. This technique is especially useful for finding circumbinary planets, which orbit around both stars of the binary system in a p-type (planetary-type) orbit.

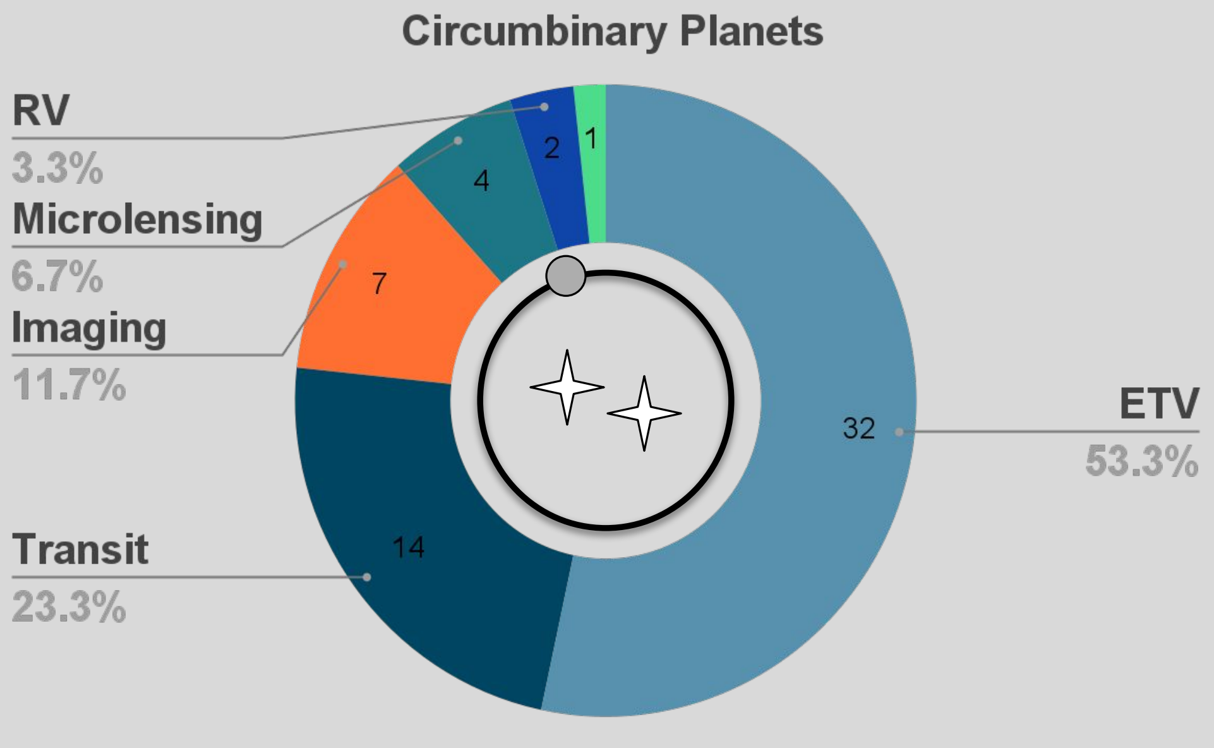

More than half of the 60 circumbinary planets detected so far have been discovered via the eclipse timing variation method.

The ETV method is biased towards detecting objects with high masses and long orbital periods. This parameter range is also covered by other detection methods, especially radial velocity, microlensing, astrometry, and direct imaging, which differ mostly in orbital inclination. However, there are no cases of ETV detections being confirmed with other methods. The current process of confirmation of ETV planets relies solely on dynamical stability tests (see Baştürk et al. 2023 for further explanation).

Circumbinary detections with transit method have shorter orbital periods and are less massive compared to those detected with ETV. On the other hand, analyses of space telescope data make low mass, short period detections possible (e.g., Esmer et al. 2022, Getley et al. 2017).

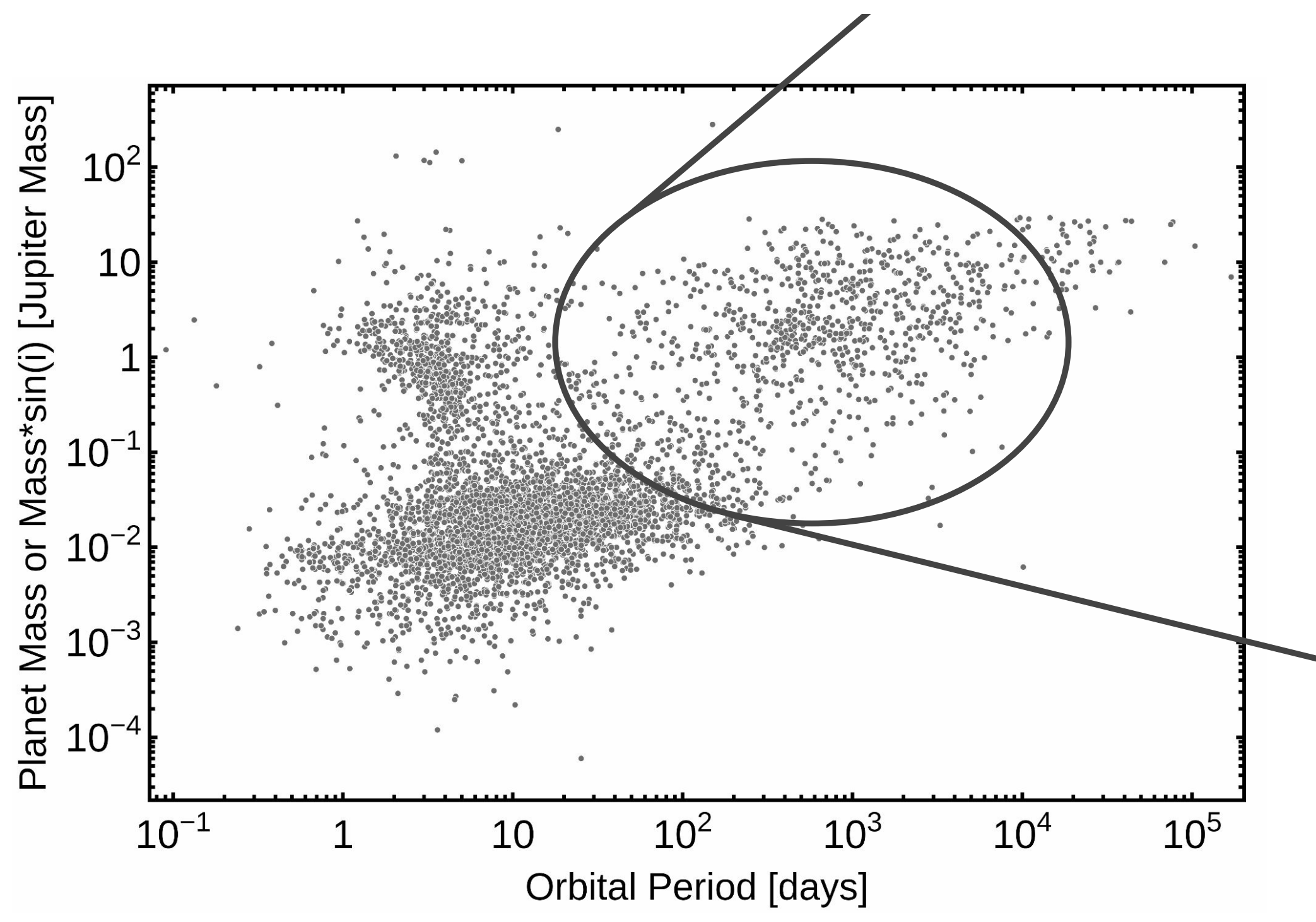

NASA Exoplanet Archive, exoplanetarchive.ipac.caltech.edu, 2024-03-29 07:23:05

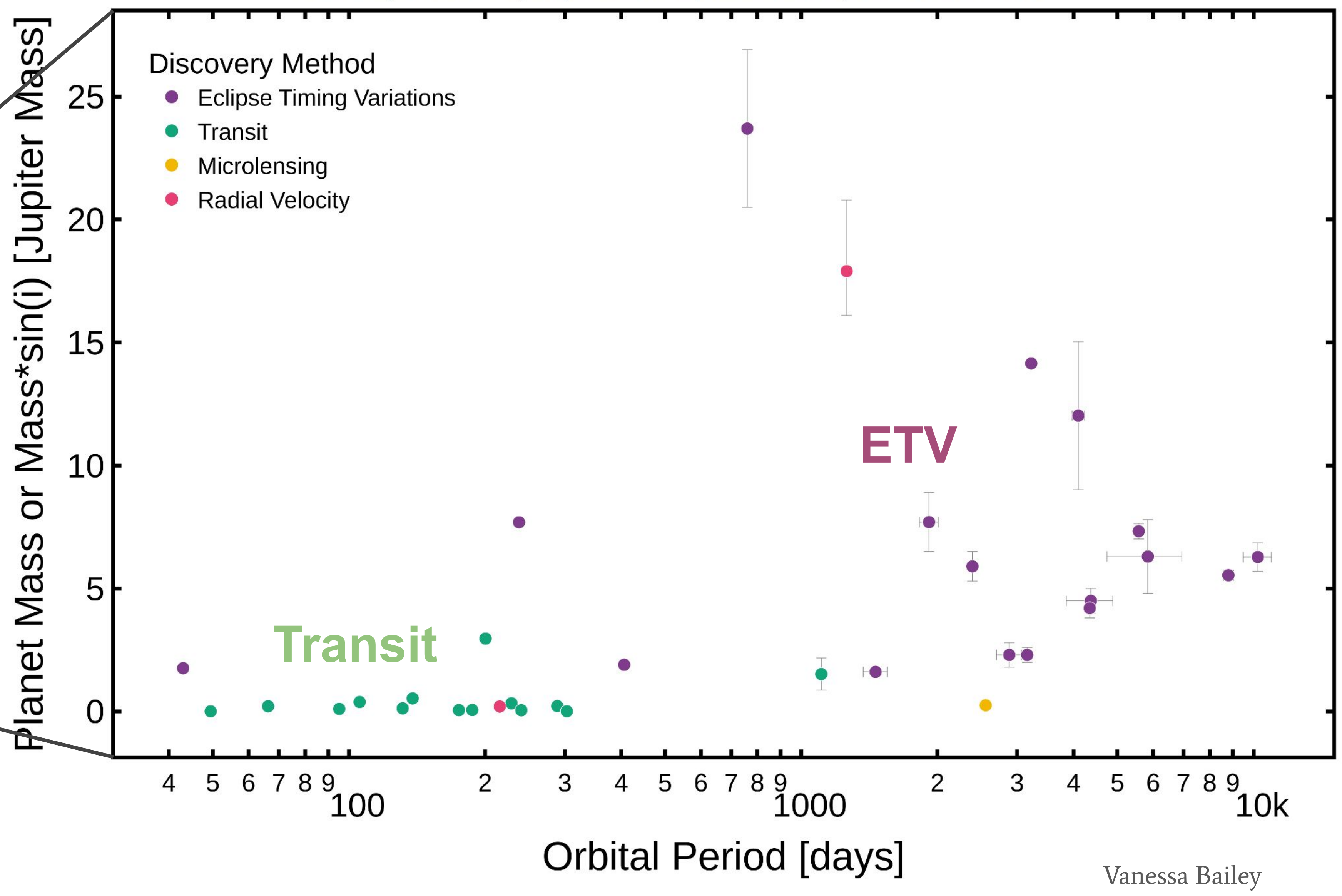

Baştürk et al. 2023

Table 1: Amplitudes of radial velocity (A_{RV}) & imaging ($A_{imaging}$) signals, and a-priori transit probabilities ($p_{tr,ecc.}$) expected from ETV systems based on planet parameters and best ETV models from the literature and assumptions of a circular orbit ($p_{tr,circ.}$).

Planet	Mass (M_{jup})	a (AU)	e	ω (°)	$R_\star$ ($R_\odot$)	P_{ETV} (years)	A_{ETV} (s)	A_{RV} (m/s)	$A_{imaging}$ (mas)	$p_{tr,ecc.}$ (%)	$p_{tr,circ.}$ (%)
DP Leo b[1]	6.05	8.19	0.39	-78.00	0.0115	28.80	66.7	155.4	47.29	0.0005	0.0007
KIC 10544976 b[2]	13.40	6.56	0.29	211.00	0.0136	16.80	80.10	308.9	24.78	0.0009	0.0010
OY Car b[3]	8.48	6.18	0	-	0.0113	14.00	65.4	222.1	135.00	-	0.00008
RR Cae b[4]	4.20	5.30	0	-	0.0155	11.90	33.9	131.1	497.13	-	0.0014
V2051 Oph b[5]	7.30	9.00	0.37	190.20	0.0103	21.64	62.2	153.9	8.94	0.0006	0.0005
DE CVn b[6]	11.50	5.75	0	-	0.0136	11.22	66.9	281.1	372.49	-	0.0011
QS Vir[7]	6.44	4.20	0.37	38.30	0.0107	7.86	21.1	177.8	161.97	0.0017	0.0012
V893 Sco [8]	9.50	4.50	0.30	-	0.0100	10.19	43.7	283.1	72.08	-	0.0010
DV UMa b[9]	26.20	8.60	0.44	26.11	0.0070	17.58	149.5	492.6	42.81	0.0006	0.0004
DD CrB b[10]	1.36	-	0	-	0.1720	10.46	9.0	51.6	15.05	-	0.0010
SDSS-1456 b[11]	16.70	-	0.05	23.70	0.0145	13.05	109.0	500.0	53.01	-	0.0008
GK Vir b[12]	0.95	7.38	0.14	198.0	0.0170	24.34	9.7	24.3	29.87	0.0010	0.0011
HW Vir b[13]	25.10	7.90	0.45	359.0						0.0128	0.0103
HW Vir c[13]	13.90	4.57	0.27	13.0	0.1750	28.21	317.0	1398.7	88.18	0.0204	0.0178
Kepler-451 b[14]	1.86	0.90	0.33	302.0						0.0856	0.1059
Kepler-451 c[14]	1.61	2.10	0.29	7.0						0.0513	0.0454
Kepler-451 d[14]	1.76	0.20	0	-	0.0205	4.93	8.9	512.8	11.75	-	0.4767
NN Ser b[15]	7.33	5.35	0.08	43.0						0.0019	0.0018
NN Ser c[15]	2.30	3.43	0.19	249.0	0.0211	16.05	67.4	305.6	21.27	0.0024	0.0029
V1828 Aql b[16]	8.00	2.90	0.52	98.0						0.0626	0.0301
V1828 Aql c[16]	2.90	1.90	0	-	0.1880	7.00	50.2	534.8	7.85	-	0.0460
NY Vir b[17]	2.78	3.39	0	-						-	0.0206
NY Vir c[17]	4.49	7.54	0.44	333.0	0.1500	27.00	56.8	238.2	24.20	0.0092	0.0093
UZ For b[18]	10.00	5.70	0.69	120.3						0.0029	0.0009
UZ For c[18]	3.22	3.00	0.45	347.4	0.0113	14.75	73.5	367.6	47.14	0.0020	0.0017
V470 Cam b[19]	28.30	3.27	0	-						-	0.0327
V470 Cam c[19]	12.40	4.71	0	-	0.2300	14.48	171.0	1672.2	7.98	-	0.0227
HU Aqr b[20]	16.80	5.48	0.23	92.3						0.0009	0.0007
HU Aqr c[20]	20.80	6.38	0.08	72.6	0.0080	19.51	181.0	857.4	77.4	0.0006	0.0006

[1]Beuermann et al. (2011), [2]Almeida et al. (2019), [3]Han et al. (2015), [4]Qian et al. (2012), [5]Qian et al. (2015), [6]Han et al. (2018), [7]Qian et al. (2010), [8]Bruch (2014), [9]Han et al. (2017), [10,11]Wolf et al. (2021), [12]Almeida et al. (2020), [13]Esmer et al. (2021), [14]Esmer et al. (2022), [15]Marsh et al. (2014), [16]Almeida et al. (2013), [17]Lee et al. (2014), [18]Khangale et al. (2019), [19]Sale et al. (2020), [20]Goździewski et al. (2015)

Vanessa Bailey
https://github.com/nasavbailey/DI-flux-ratio-plot

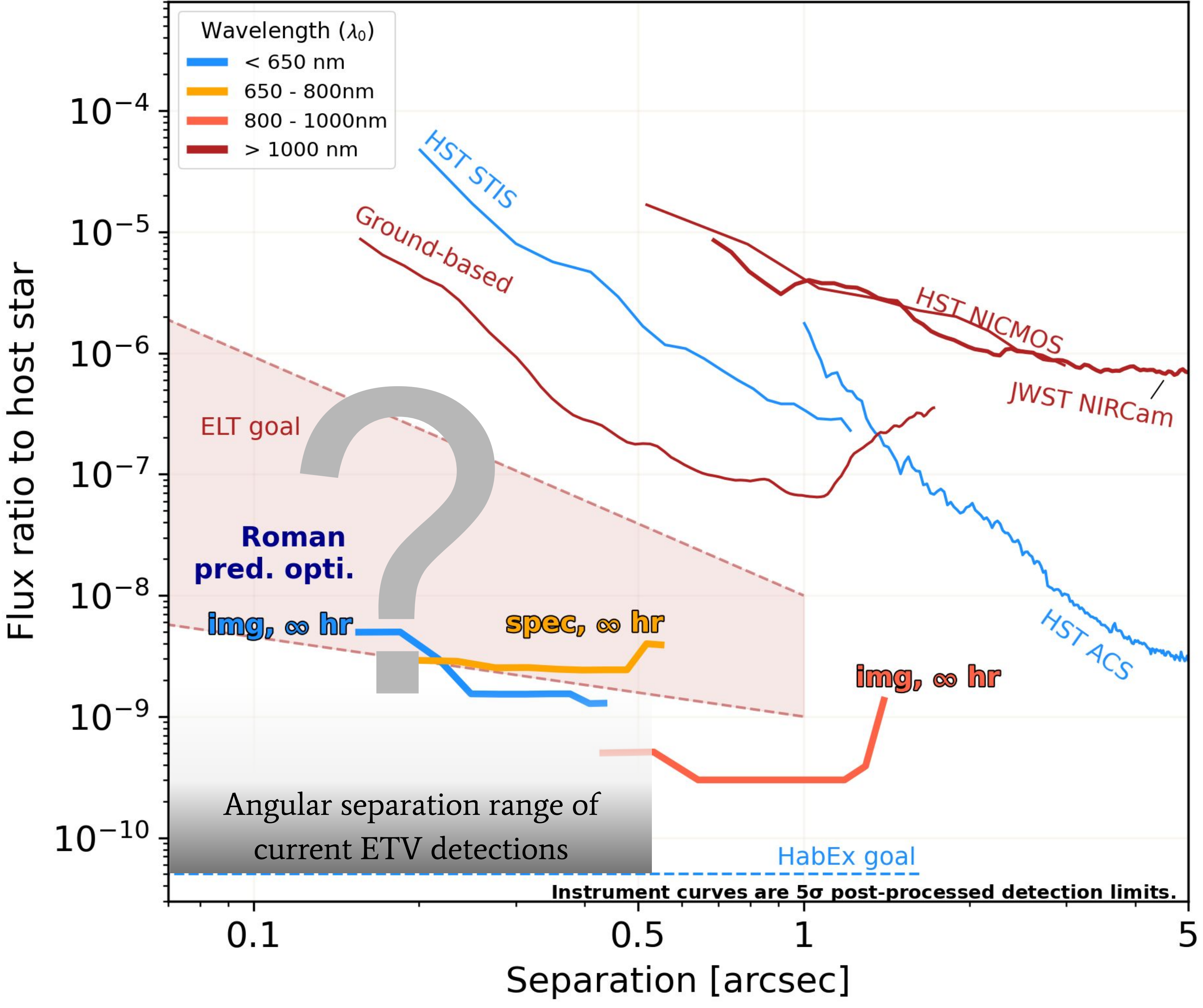

Detection with Other Methods

- The transit probabilities of ETV objects are very low. None of the known ETV objects, including those observed with Kepler or TESS data, have been confirmed through transits.
- Radial velocity amplitudes are within an achievable range. However, such confirmation requires years to decades of radial velocity follow-up observations.
- While angular separations ($A_{imaging}$ in Table 1) for imaging may be somewhat large enough, the contrasts are not well-known. Reflected light contrast should be between 10^{-8} - 10^{-10} (calculated from Currie et al. 2023), while thermal emissions are unknown. Future imaging facilities are expected to confirm ETV detections.

References

- Baştürk et al. 2023, https://doi.org/10.25518/0037-9565.11197
- Currie et al. 2023, https://arxiv.org/abs/2205.05696
- Esmer et al. 2022, https://doi.org/10.1093/mnras/stac357
- Getley et al. 2017, https://doi.org/10.1093/mnras/stx604